Alternative spectral formulations for acoustic velocity measurement

Glen C. Steyer
Structural Dynamics Research Corporation, 2000 Eastman Drive, Milford, Ohio 45150

Rajendra Singh[a] and Donald R. Houser
Department of Mechanical Engineering, The Ohio State University, 200 W. 18th Avenue, Columbus, Ohio 43210

(Received 15 August 1986; accepted for publication 3 February 1987)

The use of a multimicrophone acoustic intensity probe is investigated for the measurement of the acoustic velocity power spectrum. The conventional formulation [J. Acoust. Soc. Am. **73**, 1047–1053 (1983)] for this measurement is found to be sensitive to measurement errors. Three alternative formulations of the velocity estimate are developed that are less sensitive to random error. The various formulations are implemented into a four-microphone probe for measurement of the three velocity components. Experiments in the nearfield of a piston and a periodically stiffened plate verify the predicted relative advantages of the various estimators.

PACS numbers: 43.85.Fm, 43.20.Ye, 43.88.Kb

INTRODUCTION

In noise control and acoustical studies it is desirable to measure experimentally the acoustic intensity, velocity, and pressure spectra accurately. The introduction of the two-microphone cross-spectral density method[1] of resistive acoustic intensity measurement has provided an extremely valuable tool towards this end. This method has also been used to measure reactive acoustic intensity,[2] material acoustic impedances,[3] and acoustic radiation efficiency.[4] The latter application required the additional use of a power spectrum based method for estimation of acoustic velocity along with acoustic intensity. In this study, Forssen and Crocker[4] proposed the use of the probe in the very nearfield of a radiator to simultaneously measure the radiated sound power and surface average mean-square velocity. Close inspection of the proposed formulation for the velocity estimation reveals strong potential for error under normal test conditions. This article discusses alternative acoustic velocity formulations and how they may be implemented in a four-microphone probe to provide a more accurate velocity estimate of a three-dimensional acoustic field. Experimental results from the application of this method will be presented.

I. CONVENTIONAL SPECTRAL FORMULATIONS

The two-microphone spectral method of acoustic velocity (u) measurement utilizes the acoustic pressure (p) measured at two closely spaced microphone locations r_1 and r_2, where $r_2 - r_1 = \Delta r$, to estimate p and u at the midpoint r of the microphones. The radial velocity u_r is approximated as $u_r \cong -(1/\rho)\int(\Delta p/\Delta r)dt$. The expression for acoustic intensity (I) is then reduced to a convenient formulation in terms of the cross-power spectrum between the two microphones (G_{12}),

$$I(r;\omega) = -\operatorname{Im} G_{12}(r;\omega)/\rho\omega\Delta r, \tag{1}$$

where Im is the imaginary part, ρ is the medium density, and ω is the frequency in rad/s. Pascal[2] has shown that the reactive intensity (J), acoustic velocity power spectrum (G_{uu}), and acoustic pressure power spectrum (G_{pp}) can also be well described in terms of the auto- and cross-power spectra (G_{11}, G_{22}, and G_{12}) between the two microphones; note that $(r;\omega)$ is dropped from the spectral formulations for the sake of brevity

$$J = (G_{11} - G_{22})/(2\rho\omega\Delta r), \tag{2}$$

$$G_{pp} = (G_{11} + G_{22} + 2\operatorname{Re} G_{12})/4, \tag{3}$$

$$G_{uu_I} = (G_{11} + G_{22} - 2\operatorname{Re} G_{12})/(\rho\omega\Delta r)^2, \tag{4}$$

where Re is the real part of the G_{12}. Equation (4) presents the spectral estimator G_{uu_I} for acoustic velocity as it is normally found in literature.[2,4] By investigating the terms in Eq. (4), it becomes apparent that this estimator may be ill-formulated for the following reasons: (i) the numerator $(G_{11} + G_{22}) - 2\operatorname{Re}_{12}$ represents the difference of two quantities that are likely to be of the same order of magnitude, and (ii) the first term $(G_{11} + G_{22})$ is recognized to exhibit a bias error resulting from incoherent signal noise in the measurement channels, while the second term Re G_{12} will not exhibit such a bias error. Therefore, alternative forms of the velocity estimator are required.

II. PROPOSED SPECTRAL FORMULATIONS OF ACOUSTIC VELOCITY (G_{uu})

The first approach to an alternative estimator is developed by recognizing the relationship between pressure, velocity, and intensity

$$|p|^2|u|^2 = I^2 + J^2. \tag{5}$$

Using Eqs. (5) and (1)–(3), we now develop an alternate estimate of G_{uu} as

$$G_{uu_{II}} = \frac{I^2 + J^2}{\hat{G}_{pp}}\left(\frac{(G_{p_1p_1} - G_{p_2p_2})^2 + 4(\operatorname{Im} G_{p_1p_2})^2}{G_{p_1p_1} + G_{p_2p_2} + 2\operatorname{Re} G_{p_1p_2}}\right). \tag{6}$$

[a] Corresponding author.

 0001-4966/87/061955-07$00.80

It is interesting to note that Munro and Ingard[5] recommended an approach similar to the $G_{uu_{II}}$ estimator by including a $(\partial p/\partial x)^2$ term in the intensity estimator in the presence of a mean flow. They stated that the $(\partial p/\partial x)^2$ term "may be best expressed for numerical purposes as follows":

$$\left|\frac{\partial p}{\partial x}\right|^2 = \frac{[(|P_D|^2 - |P_u|^2)l^{-1}]^2 + 4[(\operatorname{Im} P_D P_u^*)l^{-1}]^2}{|P_D|^2 + |P_u|^2 + 2\operatorname{Re} P_D P_u^*}, \tag{7}$$

where subscripts u and D denote upstream and downstream locations, and l is the separation between microphones. This expression is seen to be essentially identical to that given by Eq. (6) for $G_{uu_{II}}$. While no explicit argument was presented by Munro and Ingard[5] for the superiority of this form, it can only be presumed that the rationale must have been along the lines previously discussed in Sec. I relative to the error of differenced quantities. While Eq. (6) does contain differenced terms, these differenced quantities are similar in nature (i.e., they are both auto-power spectra).

Now we consider the possibility of incoherent noise present in both measurement channels. The coherence function γ_{12}^2 between microphone signals p_1 and p_2 is

$$\gamma_{12}^2 = |G_{12}|^2/G_{11}G_{22}, \quad 0 \leqslant \gamma_{12}^2 \leqslant 1.0. \tag{8}$$

Using Eqs. (6) and (8) we get

$$G_{uu_{II}} = \frac{[G_{11}^2 - 2G_{11}G_{22} + G_{22}^2 + 4(\operatorname{Im} G_{12})^2 + 4G_{11}G_{22} - 4|G_{12}|^2(1/\gamma_{12}^2)]}{(\rho\omega\Delta r)^2(G_{11} + G_{22} + 2\operatorname{Re} G_{12})}$$
$$= \frac{1}{(\rho\omega\Delta r)^2}\left((G_{11} + G_{22} - 2\operatorname{Re} G_{12})\frac{-4|G_{12}|^2(1/\gamma_{12}^2 - 1)}{G_{11} + G_{22} + 2\operatorname{Re} G_{12}}\right). \tag{9}$$

Now we can compare G_{uu_I} and $G_{uu_{II}}$ by making use of Eqs. (4) and (9)

$$G_{uu_{II}} = G_{uu_I} - \frac{4(1 - \gamma_{12}^2)G_{11}G_{22}}{(\rho\omega\Delta r)^2(G_{11} + G_{22} + 2\operatorname{Re} G_{12})}. \tag{10}$$

Further, Eq. (10) can be approximated as

$$G_{uu_{II}} = G_{uu_I} - \frac{(1 - \gamma_{12}^2)G_{pp}}{(\rho\omega\Delta r)^2}. \tag{11}$$

We note that $G_{uu_{II}} = G_{uu_I}$ when $\gamma_{12}^2 = 1.0$. However, for lower values of γ_{12}^2, $G_{uu_{II}} < G_{uu_I}$. Hence, we note that the $G_{uu_{II}}$ estimator will allow a lower sensitivity to error in the velocity measurement from noise-induced bias in the auto-power spectral estimates. However, this reduced sensitivity is gained at a cost since $G_{uu_{II}}$ will exhibit a bias error when used in an acoustic field where more than one independent random acoustic source is present. For example, consider two incoherent plane waves of equal amplitudes and traveling in opposite directions. In this case, the average I or J at any point is identically zero; thus $G_{uu_{II}} = 0$. But, the actual G_{uu} is in fact twice the acoustic velocity power spectrum for each individual source. For such measurement situations, G_{uu_I} is clearly a much better choice, since it gives the correct result. The use of the $G_{uu_{II}}$ estimator should be limited to instances where the acoustic field is expected to be fully coherent spatially (i.e., either purely harmonic or characterized by a uni-modal random variable). With this limitation $G_{uu_{II}}$ would not be appropriate to use in the farfield of a source placed in a reverberant environment, but certainly would be acceptable as a surface velocity estimator in the very nearfield of a radiator.

A second limitation in both G_{uu_I} and $G_{uu_{II}}$ can be recognized for the case when acoustic measurements are made in the presence of ambient flow turbulence, for instance within an air duct or on a machine surface cooled by a fan. The turbulence in the air will result in local pressure fluctuations, which are not normally associated with an acoustic disturbance and will generally exhibit relatively little coherence between two microphones spaced sufficiently far apart.

Bolleter[6] discusses a signal processing technique that reduces the effect of the incoherent turbulence signals. This approach requires the three pressure transducers to be spaced sufficiently far apart such that the turbulence pressure at the three locations will be incoherent, yet sufficiently close so that the finite difference velocity approximation is still accurate. The acoustic pressure G_{pp} at microphone 1 is then taken to be that portion of the total G_{pp} that is fully coherent with the pressure at microphones 2 and 3. The auto-power spectral estimates for microphone locations 1 and 2 are shown below, with reference to location 3

$$G'_{11} = G_{12}^* G_{13}/G_{23}, \quad G'_{22} = G_{23}G_{12}/G_{13}. \tag{12}$$

Equations (12) may be substituted for G_{11} and G_{22} in the G_{uu_I} and $G_{uu_{II}}$ estimators. This will result in two new estimators $G_{uu_{III}}$, and $G_{uu_{IV}}$, which are summarized in Table I. It is important to note that the $G_{uu_{III}}$ and $G_{uu_{IV}}$ estimators suffer from similar deficiencies as the $G_{uu_{II}}$ estimator. Thus they also should be of limited use in a spatially incoherent acoustic field. Application of these estimators to a multimodal

TABLE I. Compilation of alternative power spectrum estimators.

Estimator	Right-hand side of equation
G_{uu_I}	$\frac{1}{(\rho_0\omega\Delta r)^2}(G_{11} + G_{22} - 2\operatorname{Re} G_{12})$
$G_{uu_{II}}$	$\frac{1}{(\rho_0\omega\Delta r)^2}\left(\frac{(G_{11} - G_{22})^2 + 4(\operatorname{Im} G_{12})^2}{G_{11} + G_{22} + 2\operatorname{Re} G_{12}}\right)$
$G_{uu_{III}}$	$\frac{1}{(\rho_0\omega\Delta r)^2}\left(\left\|\frac{G_{12}^* G_{13}}{G_{23}}\right\| + \left\|\frac{G_{12}G_{23}}{G_{13}}\right\| - 2\operatorname{Re} G_{12}\right)$
$G_{uu_{IV}}$	$\frac{1}{(\rho_0\omega\Delta r)^2}\left(\frac{\left(\left\|\frac{G_{12}^* G_{13}}{G_{23}}\right\| - \left\|\frac{G_{12}G_{23}}{G_{13}}\right\|\right)^2 + 4(\operatorname{Im} G_{12})^2}{G_{11} + G_{22} + 2\operatorname{Re} G_{12}}\right)$

random field will result in significant underprediction of the acoustic velocity.

III. IMPLEMENTATION INTO A MULTIMICROPHONE PROBE

The intensity and velocity estimators were implemented with a four-microphone probe for simultaneous measurement of the intensity and velocity components in the three Cartesian directions. In designing such a probe there are many considerations such as convenience of use, probe induced scattering effects, and accuracy of the estimate. After accounting for all of these considerations, a probe design was chosen in which the microphones were located at the apices of a quadrahedron as shown in Fig. 1.

For a microphone arrangement as shown in Fig. 1 there are six microphone pair combinations. The three components of intensity and velocity are overdetermined; thus it is recognized that there exist many possible approaches for performing the calculations, each using an appropriate weighting of these six combinations to produce the desired result. One criterion that limits these choices is that it is desirable to have the effective center of the acoustic calculation located at a common center for all measurements. This would require taking a proper weighting of the signals from all microphones to achieve this center. However, one other consideration that alters this process is that the probe is primarily intended for use in the very nearfield of a structure to estimate the surface velocity levels. Since the evanescent waves near a structure decrease rapidly with distance, it is thus desirable that for estimates of the x- and z-directed vectors, only the microphones 1, 2, and 3 be used. This will allow the effective center of the estimate to be made as close as possible to the structure's surface. The resistive and reactive acoustic intensity components and the acoustic pressure power spectrum are then estimated as follows:

$$I_x = (1/\rho\omega\Delta r\sqrt{3})(-\operatorname{Im} G_{12} - \operatorname{Im} G_{13}),$$
$$I_z = (1/\rho\omega\Delta r3)(2\operatorname{Im} G_{13} - 2\operatorname{Im} G_{12} + \operatorname{Im} G_{23}), \quad (13)$$

Microphone	Location		
	X	Y	Z
1	$\sqrt{1/3}$	0	0
2	$-\sqrt{1/12}$	−0.5	0
3	$-\sqrt{1/12}$	0.5	0
4	0	0	$\sqrt{2/3}$

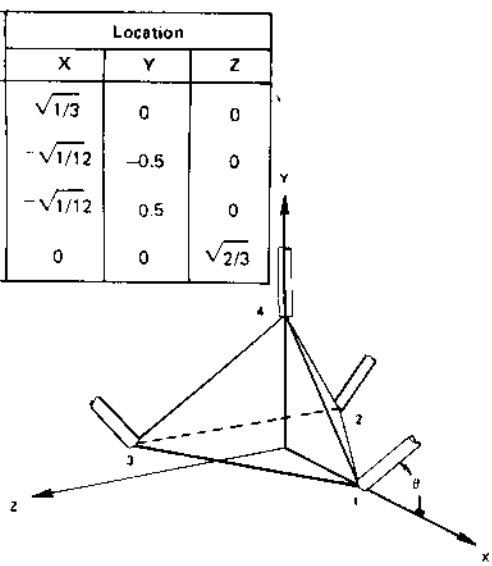

FIG. 1. Placement of microphones in a quadrahedron 3-D probe.

$$I_y = (1/\rho\omega\Delta r\sqrt{6})(\operatorname{Im} G_{14} + \operatorname{Im} G_{24} + \operatorname{Im} G_{34}),$$
$$J_x = (1/\rho\omega\Delta r2\sqrt{3})(G_{22} + G_{33} - 2G_{11}),$$
$$J_z = (1/\rho\omega\Delta r2)(G_{33} - G_{22}), \quad (14)$$
$$J_y = (1/\rho\omega\Delta r2\sqrt{6})(3G_{44} - G_{11} - G_{22} - G_{33}),$$
$$G_{pp} = \tfrac{1}{4}(G_{11} + G_{22} + G_{33} + G_{44}). \quad (15)$$

The acoustic velocity estimators were computed from the following equations:

$$G_{uu,z_I} = (\rho\omega\Delta r)^{-2}(G_{22} + G_{33} - 2\operatorname{Re} G_{23}),$$
$$G_{uu,x_I} = 3(\rho\omega\Delta r)^{-2}[2(2G_{11} + G_{22} + G_{33} - 2\operatorname{Re} G_{12} - 2\operatorname{Re} G_{13}) - \hat{G}_{uu,z}], \quad (16)$$
$$G_{uu,y_I} = 4(\rho\omega\Delta r)^{-2}[2(G_{11} + G_{22} + G_{33} + 3G_{44} - 2\operatorname{Re} G_{24} - \operatorname{Re} G_{34}) - \hat{G}_{uu,z} - \hat{G}_{uu,x}].$$

$$G_{uu,x_{II}} = (\hat{I}_x^2 + \hat{J}_x^2)/G_{pp},$$
$$G_{uu,y_{II}} = (\hat{I}_y^2 + \hat{J}_y^2)/\hat{G}_{pp}, \quad (17)$$
$$G_{uu,z_{II}} = (\hat{I}_z^2 + \hat{J}_z^2)/\hat{G}_{pp}.$$

For the remaining velocity estimators, the coherent microphone power spectra were calculated from the following equations that were then substituted into the appropriate locations in Eqs. (16) and (17) to result in $G_{uu_{III}}$ and $G_{uu_{IV}}$ estimators:

$$\hat{G}'_{11} = \left|\frac{G_{13}G^*_{12}}{G_{23}}\right|, \quad \hat{G}'_{22} = \left|\frac{G_{23}G_{12}}{G_{13}}\right|,$$
$$\hat{G}'_{33} = \left|\frac{G_{13}G^*_{23}}{G_{12}}\right|, \quad (18)$$

where superscript * denotes complex configuration.

IV. EXPERIMENTAL EVALUATION

Experimental measurements were performed in order to compare the relative accuracy of the four velocity estimators under various conditions. The first series of measurements was performed on a simple baffled circular piston. The measurements were first conducted in an ideal situation with no background noise, then repeated in the vicinity of a contaminating noise source.

After successful application to the circular piston, the measurements were performed on a plate weldment. This structure was unbaffled, and designed to be a periodically stiffened structure, similar to what might be typically found in a machine structure. Again, the relative merits of the alternative estimators were evaluated.

For these tests, a three-dimensional probe was constructed using four 12-mm ($\frac{1}{2}$-in.) condenser microphones. The probes were mounted in a holder that allowed the microphone center-to-center distances to be adjusted. The microphones were arranged in a quadrahedron scheme. A multichannel frequency analyzer was used to acquire the data and generate the averaged cross-spectral matrix for all four microphones. These matrices were stored on a hard disk and then transferred to a minicomputer for final analysis. Thus the same experimental data were used to apply each of the four alternative velocity estimators.

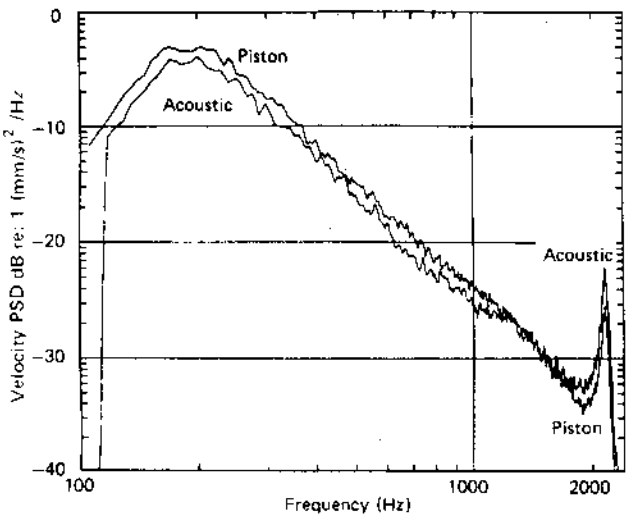

FIG. 2. Piston center velocity PSD G_{uu_a} and the measured acoustic velocity G_{uu_1} at piston center with a probe standoff distance of 12 mm.

A. Piston tests

Initial tests were performed on a baffled circular piston, made of aluminum, 200 mm in diameter, and 35 mm thick. The baffle was a 2.4-×1.2-m rectangle, and constructed from 20-mm-thick plywood. The piston was driven in the center by a 227 N (50 lb_f) electromagnetic shaker with a broadband random noise signal. Data were acquired and analyzed over a frequency range of 100–3000 Hz. However, the system anti-aliasing filters were set at 2400 Hz.

Acoustic velocity was measured with the probe centered 10 mm above the center of the piston with a probe microphone spacing of $\Delta r = 12$ mm. Figure 2 shows the structural velocity G_{uu_a}, measured using an accelerometer and acoustic velocity estimators G_{uu_1}, $G_{uu_{II}}$, $G_{uu_{III}}$, and $G_{uu_{IV}}$. All four estimators lay over each other with excellent agreement. This is due to the fact that the coherence γ^2 between the four microphones was unity for this test. This figure shows that the acoustic velocity is approximately 1 dB below the struc-

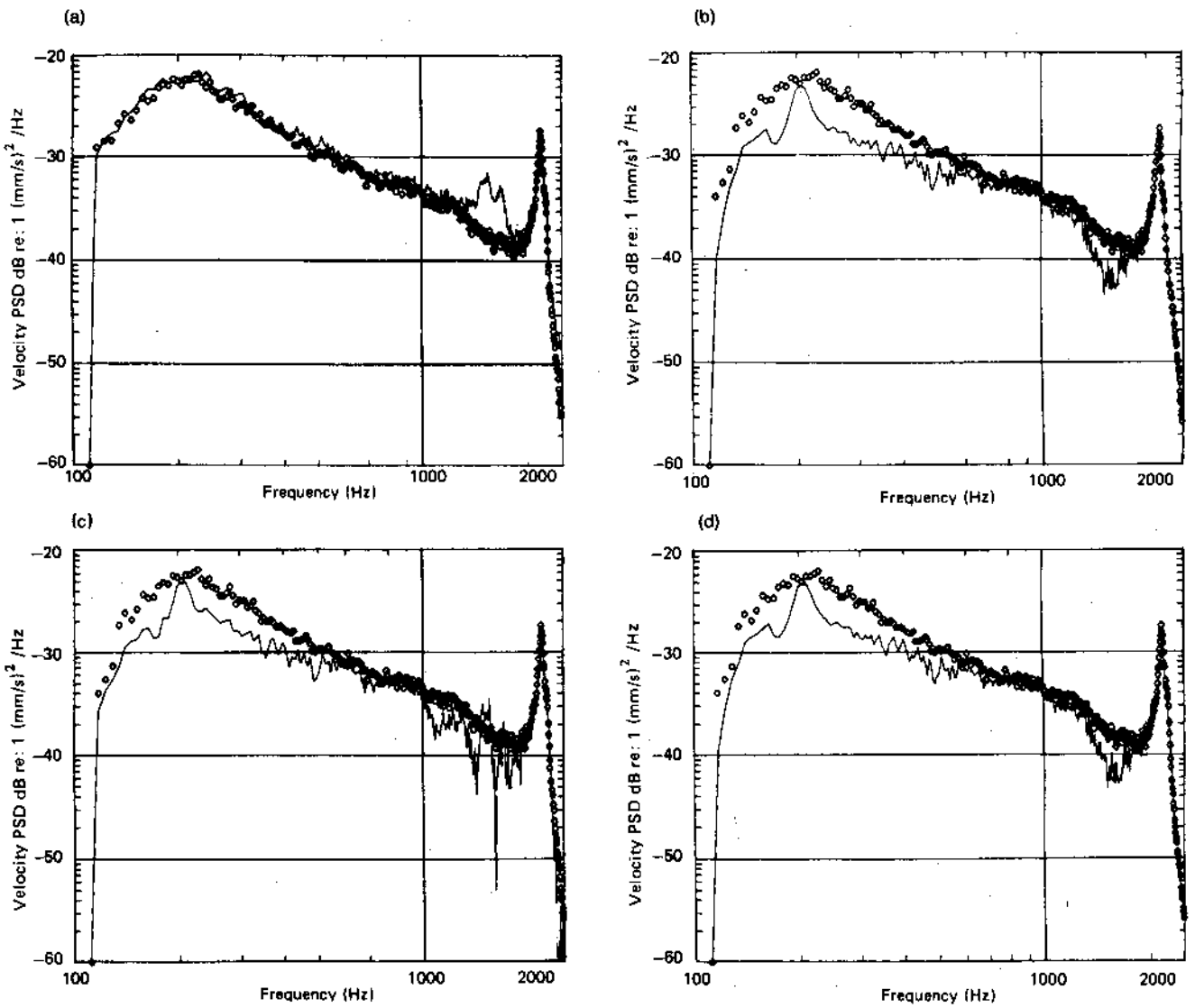

FIG. 3. Measured acoustic velocity PSD G_{uu} with and without background noise. Without background, circles (oooo); with background, line (—). (a) G_{uu_1}, (b) $G_{uu_{II}}$, (c) $G_{uu_{III}}$, (d) $G_{uu_{IV}}$.

tural velocity for frequencies below 1000 Hz. A detailed investigation determined that this difference can be accounted for by the difference in surface velocity and acoustic velocity at the center of the probes for a piston source. For frequencies above 1000 Hz the acoustic velocity G_{uu} is higher than the structural velocity G_{uu_a}, however, it was determined that in this frequency range the piston was no longer rigid with the outer part experiencing considerably higher vibrations than the center. Thus the probe is apparently experiencing increased acoustic velocity from the increased rim motion.

In order to evaluate the sensitivity of the measured velocity to background noise, the tests were repeated with an uncorrelated sound source, a speaker in the vicinity of the piston. For this test the piston was unbaffled. The speaker was driven by a broadband random signal that was incoherent with the piston motion. The speaker level was adjusted such that the acoustic pressures at the center of the piston were approximately equal for either source.

Figure 3(a) shows the acoustic velocity power spectrum for the G_{uu_1} estimator with and without background noise. This shows very little difference except in the high-frequency range around 1300 Hz. The background noise increased the measured velocity by approximately 5 dB. Figure 3(b)–(d) shows the data for the other three estimators. These estimators acted similarly to each other. For all three the indicated acoustic velocity was reduced as a result of the background noise. Furthermore, each of these estimators showed a more accurate estimate in the high-frequency range over that of G_{uu_1}. However, this was at the cost of approximately a 3–4-dB underprediction in the very low-frequency range. These results are consistent with the predicted behavior.

B. Periodically stiffened plate structure

The second example case for experimental study was a periodically stiffened plate. The structure is schematically shown in Fig. 4. The plate was constructed of a 4-mm-thick steel plate of size 430×140 mm. Stiffeners were placed around the plate perimeter and at four equally spaced locations across the plate width. These stiffeners were made from the same plate and were 30 mm deep. The plate was thus divided into five equal cells. Masses were added to each of these cells to reduce the fundamental plate cell natural frequency to approximately 500 Hz; the first few measured natural frequencies and modes are also shown in Fig. 4.

This structure was excited at a stiffener (cell No. 4) as shown in Fig. 4. The plate was otherwise in a free–free, unbaffled state. The intensity probe was used to perform measurements at the center of the structure. An accelerometer was used to measure the plate velocity at the same location.

Figure 5(a) shows the plate velocity G_{uu_a} as measured by the accelerometer, along with the velocity estimate G_{uu_1}. For this test the microphones were 14 mm apart, and the centroid of the microphones was approximately 20 mm above the plate. Figure 5(b)–(d) also shows the data for the $G_{uu_{II}}$, $G_{uu_{III}}$, and $G_{uu_{IV}}$ estimators. Results are also summarized in Table II for four specific frequencies. We note that the acoustic velocity estimate for frequencies of 500 Hz and

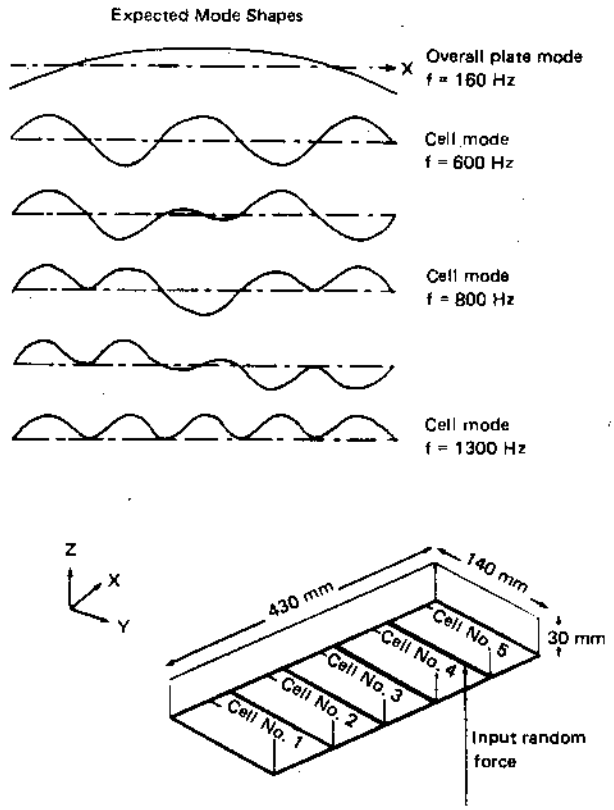

FIG. 4. Schematic of the periodically stiffened plate structure and vibration mode shapes.

higher was significantly lower than G_{uu_a}. This discrepancy can be explained by the evanescent nature of the acoustic field and will be the subject of a future article.

For frequencies above 500 Hz, all four velocity estimators provide virtually identical results. However, at frequencies lower than 500 Hz there are significant differences. From Fig. 5(a) the G_{uu_1} estimator is seen to give higher velocities below 500 Hz than those measured at the plate with an accelerometer. Furthermore, the spectral definition of the first mode at 160 Hz is significantly lost. The other three estimators are seen to provide much more accurate velocity estimation for this mode. This is consistent with the anticipated difference between the various formulations. The G_{uu_1} estimator shows the sensitivity to bias error in the low-frequency, low-signal amplitude region of the data.

V. SUMMARY

The use of a multimicrophone acoustic intensity probe was investigated for the purpose of providing a velocity power spectrum estimate. It was determined that the standard formulation for the velocity power spectrum is sensitive to measurement error. Alternative formulations were developed and implemented for a four-microphone probe to simultaneously measure the three components of intensity and acoustic velocity. Experimental measurements successfully demonstrated the anticipated measurement errors for

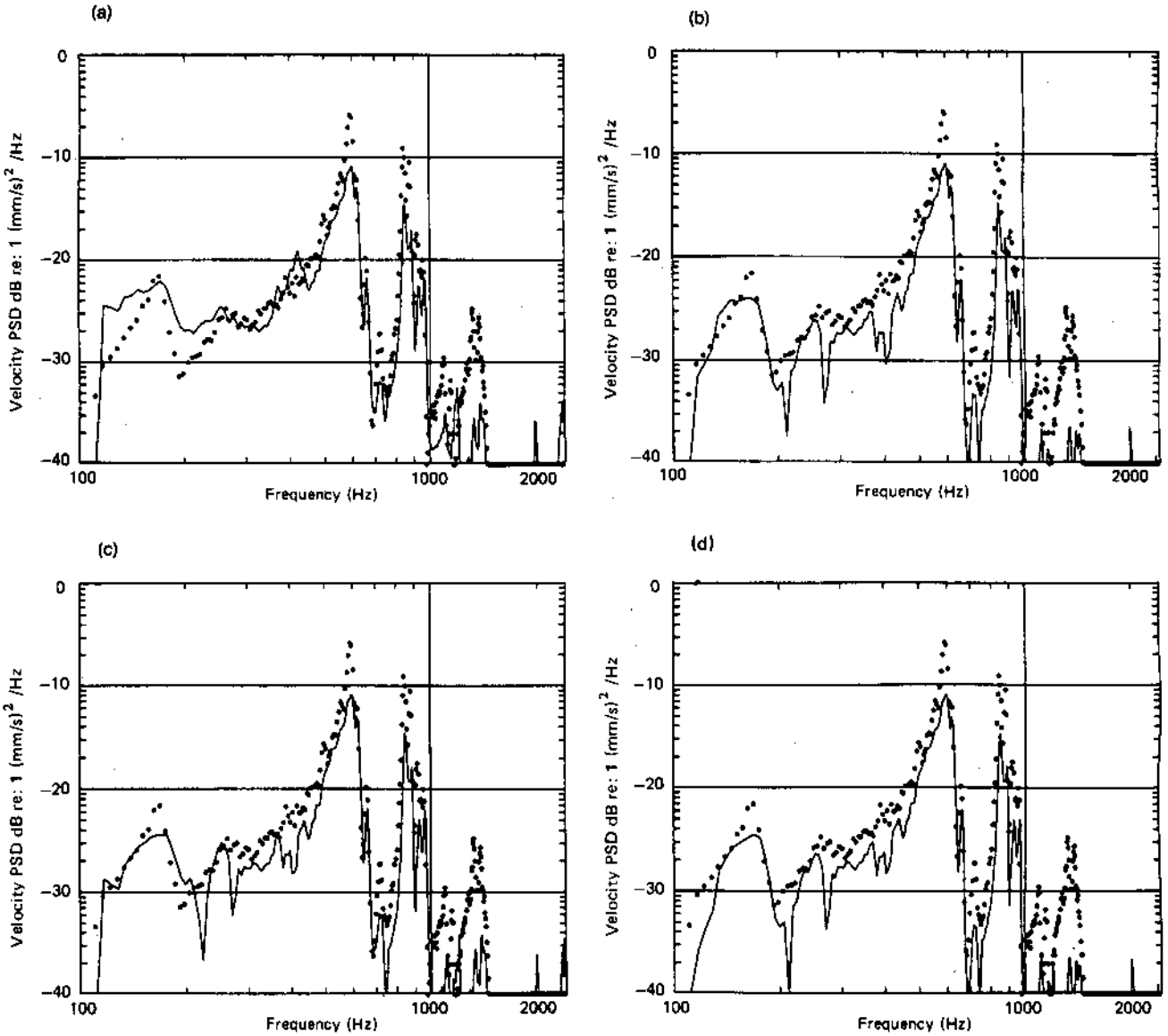

FIG. 5. Measured plate velocity G_{uu_n} (circles) and acoustic velocity G_{uu} (solid line) for the periodic plate. (a) G_{uu_I}, (b) $G_{uu_{II}}$, (c) $G_{uu_{III}}$, (d) $G_{uu_{IV}}$.

the conventional velocity formulation G_{uu_I}, $G_{uu_{II}}$, $G_{uu_{III}}$, and $G_{uu_{IV}}$. Furthermore, these tests showed the alternative velocity estimators to give a lower velocity estimate that was in certain instances more accurate.

TABLE II. Comparison of difference between measured structural velocity G_{uu_n} and measured acoustic velocity G_{uu} for the periodic plate at specific frequencies.

	120 Hz	600 Hz	800 Hz	1300 Hz
G_{uu_n} (dB *re*: 1 (mm/s)^2/Hz)	−28	−4	−9	−25
$G_{uu_n} - G_{uu_I}$	3	5	5	12
$G_{uu_n} - G_{uu_{II}}$	0	For these frequencies the four estimators gave essentially identical results.		
$G_{uu_n} - G_{uu_{III}}$	0			
$G_{uu_n} - G_{uu_{IV}}$	−1			

From the tests performed with the velocity estimators it was shown to be of benefit to provide two separate velocity estimators. Thus the use of G_{uu_I}, in conjunction with either $G_{uu_{II}}$, $G_{uu_{III}}$, or $G_{uu_{IV}}$ will result in a pseudo upper and lower bound to the estimate of velocity. In an ideal measurement situation these two estimators will converge. However, in a nonideal environment the two estimators may be used to identify the potential measurement error. The alternative estimators are proposed only for very special measurement situations such as for measurement of surface velocities, and should not be used in a general reverberant acoustic environment. When properly used, the alternative velocity estimators have already proven to be very valuable.

The use of this probe in the very nearfield of several radiators for the purpose of measuring surface velocities has shown that while an accurate measurement of acoustic velocity is possible, very considerable errors may result due to the evanescent nature of the acoustic field immediately adjacent to a structure. This will be the subject of a future article.

[1]F. J. Fahy, "Measurement of acoustic intensity using the cross-spectral density of two microphone signals," J. Acoust. Soc. Am. **62**, 1057–1059 (1977).
[2]J. C. Pascal, "Mesure de l'intensité active et reactive dans differents champs acoustiques," in *Proceedings of the International Congress on Recent Developments in Acoustic Intensity Measurement* (CETIM, Senlis, France, 1981), pp. 11–19.
[3]A. F. Seybert and T. L. Parrott, "Impedance measurement using a two microphone random excitation method," NASA Tech. Memo. 78785 (October 1978).
[4]B. Forssen and M. J. Crocker, "Estimation of acoustic velocity, surface velocity and radiation efficiency by use of the two-microphone technique," J. Acoust. Soc. Am. **73**, 1047–1053 (1983).
[5]D. H. Munro and K. U. Ingard, "On acoustic intensity measurements in the presence of mean flow," J. Acoust. Soc. Am. **65**, 1402–1406 (1979).
[6]U. Bolleter, "Using transfer function measurements to determine energy propagation in fluid lines with applications to centrifugal pump systems," in Ref. 2, pp. 261–266.